# Optimization-oriented modelling of Neutral Beam Injection for EU pulsed DEMO

**P. Vincenzi[1], P. Agostinetti[1], J.F. Artaud[2], T. Bolzonella[1], T. Kurki-Suonio[3], M. Mattei[4,5], M. Vallar[1,§] and J. Varje[3,$]**

[1] Consorzio RFX, Corso Stati Uniti 4, 35127 Padova, Italy
[2] CEA, IRFM, F-13108 Saint Paul Lez Durance, France
[3] Department of Applied Physics, Aalto University, FI-00076 Aalto, Finland
[4] Ass. CREATE-ENEA, Seconda Università di Napoli, Naples, Italy
[5] CREATE Consortium, Italy
§ Present affiliation: Ecole Polytechnique Fédérale de Lausanne (EPFL), Swiss Plasma Center (SPC), CH-1015 Lausanne, Switzerland
$ Present affiliation: Tokamak Energy Ltd, 120A Olympic Avenue, Milton Park, Abingdon, OX14 4SA, United Kingdom

E-mail: pietro.vincenzi@igi.cnr.it

## Abstract

Neutral Beam Injection (NBI) is one of the auxiliary power systems considered for EU DEMO pulsed plasma ("DEMO1"). In this paper we discuss the characteristics of an optimized NBI in terms of DEMO1 requirements, relating physics and engineering contexts, in a novel parameter range with respect to current NBI systems and in a larger plasma volume than ITER. Different injection options are investigated to account for various concepts discussed in the literature. The study is carried out through wide-range sensitivity studies by means of METIS 0.5D transport code, and ASCOT Monte Carlo simulations of injected neutral-beam particles. This investigation generated a series of recommendations for the NBI design, contributing to the system optimization process. We show how a tangential injection, aimed at plasma core, with energy $\gtrsim$ 800 keV is recommended to maintain high fusion power performance and fulfil the requirement of bulk heating. To comply with engineering constraints on NBI design, e.g. lowest interference with machine elements or compatibility with solutions for the beam-line components, imposes some restrictions when discussing the beam geometry. The minimum density, at which a NBI can be safely operated without harmful shine-through losses, is investigated for different injection energies and compared to the ITER case. The NBI operational window for DEMO is shown to be significantly extended to transient, low-density phases, highlighting also the importance of NBI systems designed for modular energy and power output. NBI can therefore sustain the plasma during a considerable part of transient phases, i.e. current ramp-up and ramp-down phases. The final decision on DEMO heating mix will be made on the basis of system operability and performance: optimized NBI is shown to be a suitable and effective option for EU DEMO inductive scenario.

Keywords: DEMO, NBI, ramp-up, fast ions, ASCOT

## 1. Introduction

The design of an European DEMO tokamak has been in the pre-conceptual phase in the last years, and soon it will enter the conceptual design phase. At the moment, the baseline concept, "DEMO1", relies on a pulsed, inductive, plasma scenario [1]. Alternative solutions are being investigated as well, including e.g. a steady-state, non-inductive plasma ("Flexi-DEMO") [2] or ELMs-free scenarios [3].

The flat-top phase of DEMO1 will be considerably longer than in present-day experiments, with the aim of having a stationary, burning plasma producing a constant amount of fusion power. The main aim of heating and current-drive (H&CD) systems during flat-top is to maintain these conditions through core plasma heating [4]. Current drive is not an explicit request for the sustainment of DEMO1 flat-top plasma current, which is induced by the central solenoid. MHD mode stabilisation requires dedicated auxiliary power, likely from Electron Cyclotron Resonance Heating – ECRH. A second target of H&CD systems is to sustain the plasma during the initial and final transient phases of the discharge, namely "ramp-up" and "ramp-down" phases [5]. Given the complexity, DEMO ramp-up and ramp-down strategies are still under discussion within EUROfusion: plasma dynamics must be well controlled with the available magnetic field coils and supported by a reasonable amount of power from auxiliary heating systems. For a pulsed device as DEMO1, flux consumption during the initial phase is also important: plasma temperature evolution and, hence, its resistivity are crucial parameters. Current drive during e.g. ramp-up phase would be hence beneficial. The final choice on DEMO heating mix is still not made, and different systems are under evaluation. The decision will be also based on the system flexibility for different plasma phases, and the design of the H&CD systems has to seriously take into account plasma transient phases besides flat-top phase.

Neutral Beam Injection –NBI- has shown in the last decades to be an effective auxiliary power system. Starting with the first proof of principle of NBI heating back in the '70s [6], NBI was crucial for the discovery of the H-mode confinement in the ASDEX tokamak [7]. The fusion production records of '90s in TFTR and JET was possible thanks to NBI heating and the fusion reactions produced by beam-plasma interactions [8], [9]. NBI is currently used in almost all top experiments worldwide, with considerable power for plasma heating, current-drive and plasma rotation control. NBI will be also the main heating systems for ITER plasma, with two (or even three) injectors, having total power of $P_{NBI,tot}$ = 33 MW at the energy $E_{NBI}$ = 1 MeV. ITER high energy NBI will be based on negative ion sources. The realization of the world first 1 MeV negative-ion-based injector requires the development of a system prototype, which is currently ongoing [10]. Due to its reliability and long-lasting operational experience, NBI is one of the H&CD systems currently considered to provide auxiliary power to EU DEMO plasma [11], [12]. This work is focused on the study of NBI for DEMO1 plasma. We leave to other publications the discussion of other proposed DEMO H&CD systems, e.g. ECRH [13] and Ion Cyclotron Resonance Heating –ICRH- [14].

The design of a NBI system for DEMO is ongoing within EUROfusion, and different design options are being discussed. Many aspects of the injector have to be improved with respect to ITER NBI, as highlighted in [15]. The injector efficiency is the parameter which has to be improved most with respect to ITER (being currently only 26%), to make NBI a suitable solution for a fusion reactor. A crucial part of the NBI system determining the overall injector efficiency is the neutralizer [16], which has the task of neutralizing the negative ion beam. In ITER and present-day experiments (e.g. LHD [17]), it consists of a low efficiency gas neutralizer. R&D on alternative neutralizer concepts is ongoing: at the moment both photo-neutralization [18], [19], [20] and plasma-neutralization [21] options are being investigated for DEMO. The NBI design will have to take into account the final neutralizer choice, which can modify the beam geometrical shape. Injection energy is a parameter widely discussed too, especially for steady-state DEMO concepts ("DEMO2" steady state tokamak [22] or "Flexi-DEMO" [12]), where current drive becomes a crucial requirement for auxiliary power systems. If 800 keV (as proposed in [23]) seems to be more convenient from the system reliability point of view, 1 MeV injector has the advantage of maximizing the return of experience from ITER NBI development. At the moment, 1 MeV beam energy is the value selected for the last DEMO1 concept (2019 version) [24]. Concepts with higher energies were also proposed, up to 2 MeV [25]. We remind that, so far, the highest energy ever achieved for a NBI system has been in JT60-U, by a NBI system designed for 500 keV that reached 416 keV at maximum [26], [27]. The investigated NBI parameter range in this work extends to energies studied only for ITER case, being though DEMO plasma volume larger than all its predecessors, with implications in e.g. beam-particle ionization and losses.

The first aim of this paper is to discuss the NBI system capabilities to satisfy DEMO1 requirements, describing the physics of its interaction with DEMO1 plasma, limits and possible operational windows during the main phases of the discharge. Fast ions dynamics can be very complex, including the interaction with MHD modes: this part of physics is not treated in this paper. The present work connects the technological design studies of the DEMO NBI system to the physics and scenario modelling investigations, taking into account that H&CD system design choices and plasma scenario objectives are closely related. This link is studied in the present paper through numerical simulations of beam-plasma interaction and integrated

transport modelling. From one side, wide-range parametric studies enable the exploration of different injection options, in order to find solutions to better cope with scenario requirements, and thus helping the NBI-system technical design work. On the other side, detailed analyses of selected NBI engineering options are carried out to validate the system design work and provide precise information for DEMO plasma scenario studies. These two sides of NBI conceptual design work were iterated in a loop through years, being essential for the integrated development of an optimized NBI system for DEMO plasmas. Lastly, this paper wishes to give the author's point of view on some "frequently asked questions" on DEMO NBI, in particular:

1. What if we modify the injection angle to accommodate for DEMO machine design requests?
2. Do we need a DEMO1 NBI which can be vertically tilted during operations?
3. What if we change the injection energy? E.g. from 800 keV to 1 MeV (or even more)?
4. Given the 50:50 D:T plasma, is it useful having also a tritium NBI instead of deuterium-only NBIs?
5. Can we use NBI during DEMO ramp-up or ramp-down?

These points will be addressed throughout the paper and summarized in the conclusions.

The paper is organized as follows. Section 2 presents the modelling setup used for this work. The numerical tools are briefly described in sec. 2.1, focusing on the different capabilities of a fast, semi-analytical model versus a Monte Carlo code. Section 2.2 introduces DEMO plasma parameters and kinetic profiles employed as input for the analysis, both for flat-top and ramp-up phases. Section 2.3 presents the main characteristic of a DEMO NBI system, describing then the reference design used as starting point for the work. Section 3 introduces some basic physics concepts on beam-plasma interaction, from the point of view of a NBI system optimization: from simple considerations, the system can be already roughly sized. Section 4 describes the results of the modelling work performed for NBI during DEMO flat-top phase, first with wide parametric scans (sec. 4.1) and then with detailed Monte Carlo simulations of selected NBI designs (sec. 4.2). Section 5 focuses on the operability of NBI during the ramp-up phase, targeting the problem of shine-through losses and how to optimize NBI usage during this phase. In section 5.1 a multivariable regression for shine-through losses for DEMO-like machines is obtained, in order to allow fast estimations of NBI power losses during any low-density phase. The paper ends with a summary of the main results of this work in section 6.

## 2. Description of the modelling environment

### *2.1 Numerical codes employed for beam-plasma interaction analyses*

The modelling work presented in this paper was accomplished with two numerical codes having different characteristics. The first code is METIS [28], a 0.5D transport code, capable of simulating a full tokamak discharge within limited computational time. It uses a mix of 0D scaling laws and analytical formulas, a 1D current diffusion solver, and 2D equilibria. The code performs integrated simulations considering simplified source models, including neutral beam injection: this means that plasma parameters are evolved consistently with the effect of different actuators, such as NBI. METIS was already used for DEMO simulations in the past [5], [22], being well suited for scenario modelling and sensitivity scans.

NBI in METIS is described by up to two injectors with tunable power waveform, particle energy, injection direction and horizontal and vertical dimension of the beam. The injection line is specified by the tangency radius of the beam in the plasma ("$R_{tang}$"). There is the possibility of vertically tilting the beam thanks to a parameter ("$z_{ext}$") indicating the normalized flux coordinate on a vertical axis from the plasma centre through which the beam trajectory passes. The injection line is formed by parallel sub-beams, i.e. a beam divergence cannot be modelled. Fig. 1 describes schematically all the beam geometry settings in METIS, including beam source dimension ("drs1", "dsz1"). The ionization of the beam inside the plasma is described by an attenuation equation; heat deposition and current-drive are estimated by an analytical solution of the Fokker-Planck equation.

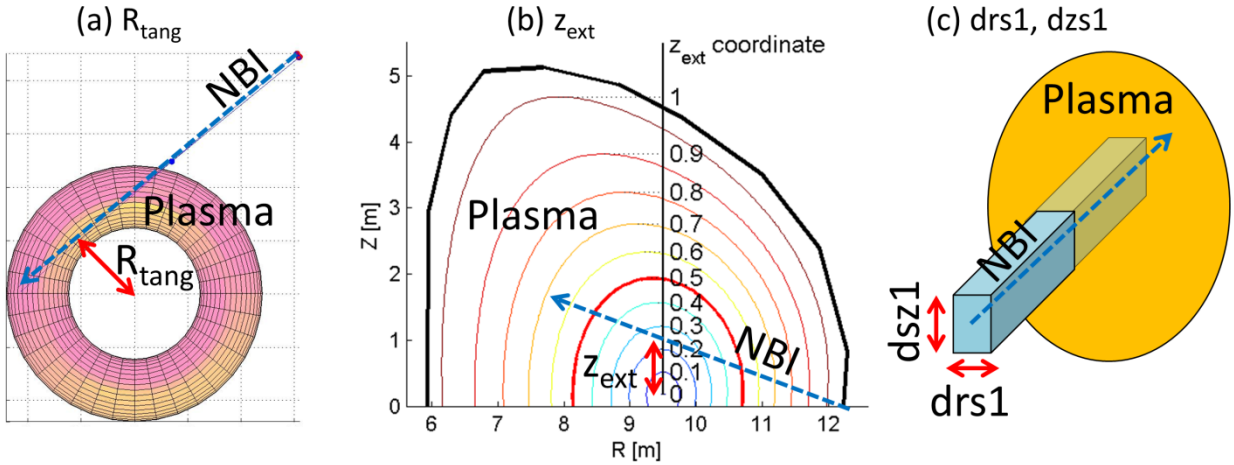


Figure 1: Schematic description of the NBI geometry input parameters in METIS: (a) the tangency radius "$R_{tang}$", depicted in the horizontal plane, (b) the vertical tilt of the beam "$z_{ext}$" in a poloidal cut of the plasma and (c) the beam horizontal dimension "drs1"and vertical dimension "dzs1".

The other code employed in the present work is ASCOT suite of Monte Carlo codes (specifically ASCOT4 version), widely used to study fast ions in plasmas. It is employed both in tokamak and stellarator studies, since it can deal with 3D magnetic fields. ASCOT solves the kinetic equations using test-particle approach [29], providing detailed information on beam particle, momentum, current and energy sources into DEMO plasma. The population of newly-born fast ions is generated for ASCOT by BBNBI Monte Carlo code [30], a beamlet based model for fast particle ionization. BBNBI calculates indeed the ionization points of the neutral beam in the plasma and counts the neutral particles which are not ionized and collide with the opposite wall ("shine-through" losses). BBNBI uses a realistic 3D geometry of the injector source, described beamlet by beamlet. All the beamlets of each source are reproduced in BBNBI as separate Gaussian beams, thus allowing the simulation of the correct beam focusing. Beamlet divergence can also be specified, as the case of this work (see section 2.3). Therefore, the representation of the NBI geometry is very accurate if compared to METIS. Moreover, a detailed 3D first wall structure can be implemented. A realistic first wall is necessary to estimate the fast particle power loads, as presented later in the paper for shine-through losses. BBNBI + ASCOT are used in this work for "stand-alone" simulations (as opposed to "integrated" simulations done with METIS), i.e. NBI acts on "frozen" plasma kinetic profiles, not modified by the injection itself. This steady-state approach is a valid approximation for slowing-down simulations also during the DEMO transient phases, due to their considerable duration: DEMO ramp-up duration is estimated in the order of hundreds of seconds [5] with respect to a few seconds of fast ion slowing down time. Accuracy of results comes at the cost of long computational time, which make Monte Carlo codes useful for detailed analysis but of limited use for wide parametric studies. For BBNBI related results (ionization profiles and shine-through losses on the 3D wall) we used one million Monte Carlo test particles, meaning that BBNBI continues to generate markers until one million particles are actually ionized in the plasma. This implies that scenarios with large shine-through losses will also have a larger number of markers and hence higher accuracy. Due to the use of ASCOT in this paper mainly for 0D outputs without a representing fast ion orbit losses on a 3D wall, we used a reduced number of markers of 50 thousands for ASCOT fast-ion slowing down calculations in order to decrease the computational time keeping a good accuracy.

During neutral beam ionization and fast ion slowing down, different mechanisms can lead to fast particle losses. We now briefly list some of the main loss processes specifying whether the codes used take them into account or not. Starting from the beam ionization, both METIS and ASCOT (through BBNBI) estimate shine-through losses. If a neutral particle is ionized before reaching the plasma, i.e. in the Scrape-Off Layer ("SOL") region, it may follow an unconfined orbit colliding eventually with divertor plates. Usually this loss channel is negligible due to the low density of SOL, but it can become important in case of high separatrix density. ASCOT, but not METIS, takes into account SOL neutral particle ionization by extrapolating 1D temperature and density profiles beyond the separatrix: SOL losses will be accounted within the more general "orbit losses" group. SOL losses were indeed shown to be negligible for DEMO [31] by means of a SOL density scan with ASCOT code. Orbit loss channel caused by open orbits is populated also by fast ions which end up after collisions into unconfined orbits. ASCOT does estimate this loss channel. On the other hand, only part of orbit losses is analytically estimated by METIS, i.e. fast ions are lost if their orbit width is less than the distance to the last closed flux surface, "LCFS", being this loss channel called fast ion "first orbit losses". METIS does not estimate orbit losses due to collisional processes.

In case of presence of neutral particles inside the plasma, charge exchange processes may neutralize fast ions, resulting in fast neutrals escaping the plasma. At the moment, neither METIS nor ASCOT take into account charge-exchange loss channel, although in DEMO, background neutrals are expected to be negligible due to low thermal neutral penetration in the plasma. The implementation of charge exchange losses estimation in ASCOT is ongoing at the moment.

The NBI modelling presented in this paper includes the whole plasma region. The fast particle losses in duct and port regions of the NBI system are excluded from the present study, assuming that, throughout the whole paper, the "NBI power" always refers to the injected power delivered to the plasma.

### *2.2 DEMO1 pulsed scenario characteristics*

DEMO1 main parameters are frequently updated (on average every one to two years) as result of the studies within the EUROfusion Power Plant Physics and Technology department. In the present work we use DEMO1 parameters as described in [4] and summarized in this section. The fact that the parameters used, shown in table 1, are not the latest one (e.g. [1]) is not of concern: the changes are too small to have any significant impact on the conclusion of this work. In particular, the aspect ratio is not changed and $B_T$ and $I_p$ flat-top values varied only little.

In this work we only consider an axisymmetric magnetic field: DEMO fast ion confinement in case of 3D non-axisymmetric magnetic background was studied in [31] and more generally in [32]. Plasma kinetic radial profiles used in this work are shown in fig. 2, for stationary, flat-top phase. We define the radial coordinate used for plasma profiles in the present work, $\rho_{pol}$, as the square root of the normalized flux ($\Psi$) of the magnetic field in the poloidal direction: $\rho_{pol} = \sqrt{\frac{\Psi_{pol}-\Psi_{pol,centre}}{\Psi_{pol,edge}-\Psi_{pol,centre}}}$. DEMO1 inductive plasma is characterized by a centrally-peaked current density profile.

| | | |
|---|---|---|
| *Major radius* | **R [m]** | 9.1 |
| *Aspect ratio* | **A=R/a** | 3.1 |
| *Plasma volume* | **Vol. [$m^3$]** | 2502 |
| *Toroidal magnetic field at $R_0$* | **$B_{T,0}$ [T]** | 5.7 |
| *Plasma current* | **$I_p$ [MA]** | 19.6 |
| *Edge safety factor* | **$q_{95}$** | 3.8 |
| *Total normalised plasma $\beta$* | **$\beta_N$** | 2.6 |
| *Vol. averaged electron density* | **$<n_{e,vol}>$ [$10^{19}$ $m^{-3}$]** | 7.9 |
| *Central electron density* | **$n_{e,0}$ [$10^{19}$ $m^{-3}$]** | 10.1 |
| *Greenwald fraction* | **$f_G$** | 1.2 |
| *Vol. averaged electron temperature* | **$<T_{e,vol}>$ [keV]** | 12.8 |
| *Central electron temperature* | **$T_{e,0}$ [keV]** | 28.5 |
| *Vol. averaged ion temperature* | **$<T_{i,vol}>$ [keV]** | 11.9 |
| *Central ion temperature* | **$T_{i,0}$ [keV]** | 25.3 |
| *Flat-top H&CD power* | **$P_{H\&CD}$ [MW]** | 50.0 |
| *Confinement factor* | **H factor** | 1.1 |
| *Effective charge* | **$Z_{eff}$** | 2.0 |
| *α-particle power* | **$P_{alpha}$ [MW]** | 398.6 |
| *Total fusion power* | **$P_{fus}$ [MW]** | 2004.0 |

Table 1: DEMO1 [4] main flat-top parameters used for this work.

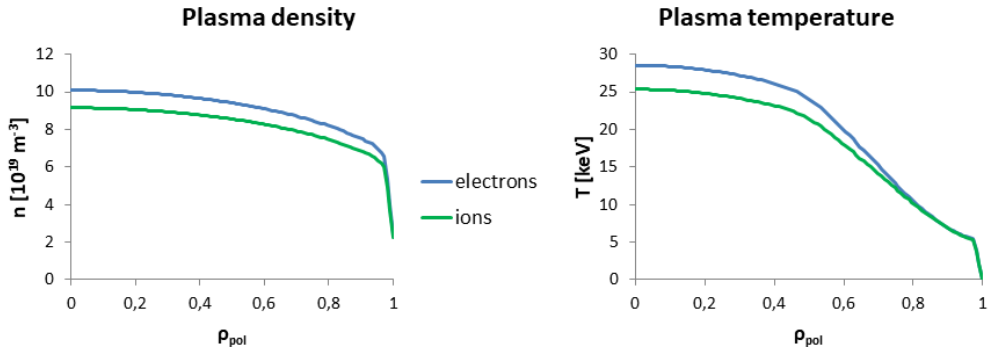


Figure 2: Plasma kinetic profiles (density – left - and temperature – right -) during plasma flat-top. In green ion profiles, in blue electron ones.

In this paper, NBI is studied also during the DEMO1 current ramp-up phase. The strategy of plasma evolution (shape, current, density, L-H transition…) during this transient phase is currently under discussion and not yet decided. To evaluate beam interaction with DEMO1 ramp-up plasma, we selected a set of snapshots of a possible plasma evolution described in [5], where additional ECRH power was used in the early phase of the discharge. The study is restricted to an already diverted plasma, starting at $I_p$ =5 MA.

In fig. 3, plasma shapes characterizing DEMO1 ramp-up from free-boundary equilibrium CREATE-NL code [33], and plasma kinetic profiles from METIS transport code [28], are shown. The total ramp-up time is ≥ 200s (≤ 100 kA/s), due to controllability issues, being ~ 2 orders of magnitude larger than typical fast ion slowing down time. The point at $I_p$ = 19.6 MA corresponds to the start of the plasma current flat-top phase: the stationary phase with the profiles shown in fig. 2 will be reached after this.

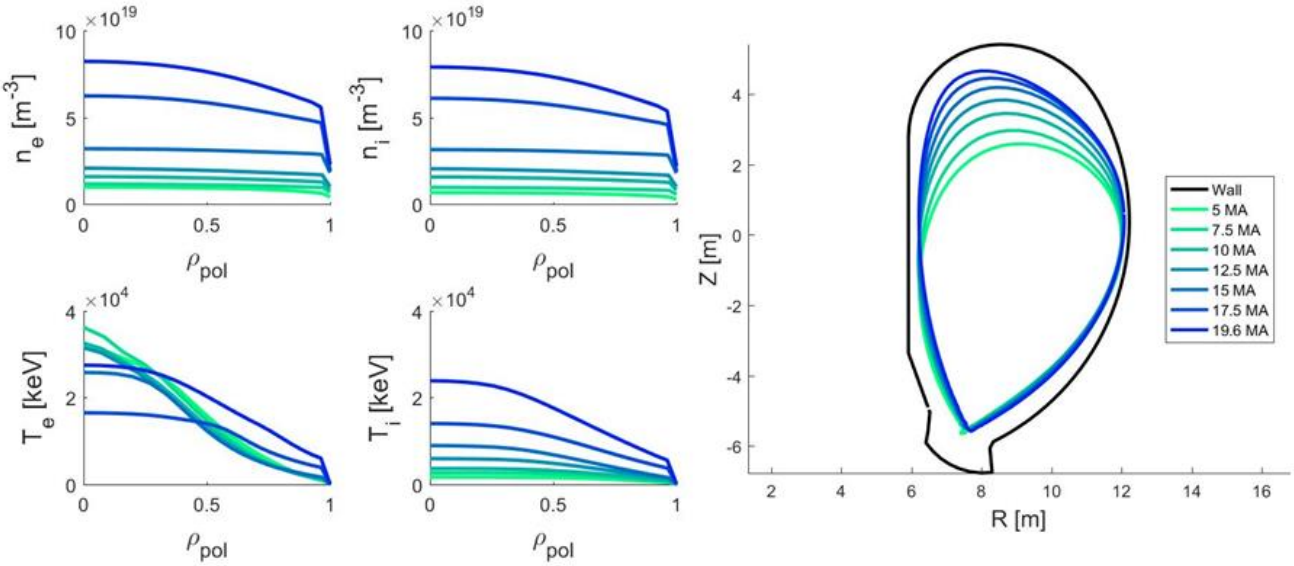


Figure 3: Evolution of plasma kinetic profiles (density – top left - and temperature – bottom left) and plasma boundaries (last closed flux surface – LCFS, right) during DEMO1 ramp-up. Profiles and boundaries are colour-coded with the corresponding plasma current $I_p$ [MA].

### *2.3 Description of DEMO NBI system*

The choice of which DEMO NBI system to consider as starting point for the present modelling work is not unique. An optimized injector design, based on negative ions, was proposed in [23], where different solutions were considered to improve the overall system efficiency. A first study comparing this DEMO NBI concept and an ITER-like NBI was performed in [34]. For detailed, orbit-following, Monte Carlo simulations of neutral beam injected particles with ASCOT, we decided to start from the geometry of DEMO NBI design of [23] as reference. We tried then to account for different options

through parametric scans of injector parameters, as described in the next sections. In particular, due to the recent modifications of DEMO NBI [24], 1 MeV injection energy case will be deeply discussed in the paper.

The NBI system we selected as reference is composed by three injectors ($P_{NBI}$ = 16.8 MW per injector, $P_{NBI,tot}$ = 50.4 MW). The injection is tangentially oriented in the direction of the plasma current ("co-current" injection). The injection energy of this system was set to 800 keV in order to improve the system-reliability of the concept, given the fact that 800 keV guarantees enough beam penetration in the plasma [34]. The NBI design proposed in [23] is indeed compatible with a photo-neutralizer, this concept having the advantage of very high neutralization efficiency and resulting in a peculiar "thin and tall" beam shape.

In table 2 the main NBI parameters relevant for this work are summarized. Each injector is made of two vertical blades, consisting of ten modular negative ion sources each, i.e. a total of 20 sources per injector. Every source produces 60 beamlets (1200 beamlets per injector in total, each of them reproduced in BBNBI code). The beam was designed to have a focus point both in the horizontal and vertical planes at the wall port in order to minimize the impact of the aperture on the breeding blanket. A single-beamlet divergence of 7 mrad is used in the simulations. A sketch of the injection lines of DEMO injectors can be found in [23].

| | | |
|---|---|---|
| *NBI power per injector* | **$P_{NBI}$ [MW]** | 16.8 |
| *Number of injectors* | **#** | 3 |
| *NBI energy* | **$E_{NBI}$ [keV]** | 800 |
| *Beam line tangency radius* | **$R_{tang}$ [m]** | 7.09 |
| *Horizontal injection angle at first wall* | **[°]** | 30 |
| *Vertical tilt of the source with respect to horizontal mid-plane* | **[°]** | 0 |
| *Beam dimensions at the source (hor. x vert.)* | **[m]** | 0.45 x 4.02 |

Table 2: main parameters of DEMO NBI proposed in [23], used as starting point for Monte Carlo modelling in this paper.

## 3. Basics physics processes relevant for NBI design and optimization

In this section we would like to review some basic considerations about beam-plasma interaction that represent the first steps of an optimization process, and help for the interpretation of the results presented in the next sections. A complete discussion of the physics treated can be found in different books (e.g. [35], [36]).

In the process of the neutral beam ionization in the plasma, "beam stopping" cross section [37] scales almost linearly with inverse of the beam energy. Therefore, the mean free path of the neutral beam in the plasma, λ, scales with $\sim E_{NBI}/n$, with n the average plasma density. As a rule of thumb, for a good beam absorption, the beam energy is usually set so that λ is of the order of *a*, the machine minor radius. For DEMO, with *a* = 3.1 m and $E_{NBI}$ = 800 - 1000 keV, λ is roughly 2 - 2.50 m. Of course, decreasing the plasma density e.g. during transient phases, the beam mean free path increases and part of the beam may not be ionized and will contribute to the shine-through losses.

A tangential injection line (better if avoiding the inner wall) increases the path of the beam in the plasma with respect to normal injection, and this helps in reducing the shine-through losses. A typical case showing large orbit losses is the counter-injection of fast particles with respect to the plasma current: unfavourable banana orbits drives the fast ions outwards. If injected tangentially, NBI can also induce current and provide torque to the plasma. Considering a beneficial current-drive, favourable fast ion orbits and reduced fast particle losses, co-current tangential injection is chosen for DEMO.

The slowing-down time, i.e. the time taken for a fast ion to thermalize by ceding its energy, depends linearly on $\frac{T_e}{n_e}$, while only logarithmically on $E_{NBI}$. For DEMO1 flat-top with $E_{NBI}$ = 800 - 1000 keV, it results ~1 s, using volume averaged plasma temperature and density described in section 2.2.

Coulomb collisions are responsible for the transfer of energy from energetic ions to background plasma (electron and ions – including impurities). The critical energy $E_c$ is a parameter which corresponds to the fast ion energy at which the collisional transfer of energy to plasma ions and electrons becomes equal. $E_c$ depends mainly on plasma electron temperature and on the NBI injected species. For D injection into D plasma, as a rule of thumb, $E_c$ [keV] = 18.6 $T_e$ [keV] [38]. Integrating over the slowing down process, if $E_{NBI} > 2.5 \cdot E_c$, then electron heating dominates, otherwise ion heating prevails. For DEMO, taking into account also the presence of tritium, $\langle E_c \rangle \sim 200$ keV, and $2.5 \cdot Ec \sim 500$ keV: with the considered injection energies, NBI power is mainly absorbed by electrons, as it will be with alpha particles (3.5 MeV). However, $E_c$ varies locally along the radius, depending linearly on $T_e$: it is lower in the edge and higher in the core. For this reason, beam fast ions will transfer more power to plasma ions in the core, where $E_{c,0} \sim 450$ keV, and significantly more power to plasma electrons in the edge. The final power distribution to plasma species will depend therefore also on the injection trajectory.

Increasing the beam energy, and therefore fast ion collisions with plasma electrons, current drive efficiency ($\eta_{NBCD}$) increases, although $\eta_{NBCD}$ has a broad maximum in energy: 90% of the maximum $\eta_{NBCD}$ is reached already at half the $E_{NBI}$ corresponding to the highest $\eta_{NBCD}$. The source of toroidal torque, linked to fast ion collisions with plasma ions, increases if $E_{NBI}$ is decreased. The effect of NBI on plasma rotation is expected though to be very low, due to the foreseen injection power, energy and the high plasma mass of DEMO. NBI is also a source of particle in the plasma, although its magnitude, depending on injected power and particle energy, has to be related to the plasma volume and to other particle sink/sources in the plasma.

## 4. Modelling of NBI options during the flat-top stationary phase

In the following analyses, NBI parameters (energy, injection geometry) were varied to investigate the beam-plasma interaction during the stationary flat-top phase of DEMO1. In particular, regarding the injection energy, we used the following values:

- 500 keV, as the designed energy for the negative-NBI system in JT60-U and JT60-SA [26], [27]
- 800 keV, as proposed for DEMO NBI in [23]
- 1 MeV, like ITER NBI [39] and 2019 DEMO NBI [24]
- 2 MeV, as an extreme case, speculated in [25]

From the technological point of view, higher injection energy relaxes the requirement on the extracted negative ion current, which is a delicate parameter. On the other hand, higher beam energy complicates the injector design and the high voltage handling. Lower beam energy than 500 keV is not considered, since it would lead to peripheral beam ionization and, thus, unsuitable beam power deposition for DEMO1 flat-top.

We first swept widely the NBI parameter space with METIS code, as reported in section 4.1. In section 4.2, we implemented in ASCOT the NBI design described in section 2.3, which complies with the engineering study presented in [23] in terms of technological feasibility: starting from this realistic design, selected NBI options are then discussed.

### *4.1 Wide range parametric study with METIS*

A first wide scan of NBI injection geometry using PENCIL analytical code [40] was performed for DEMO in [41], discussing the best solutions for the NBI system. In the present study, we analyse a more recent plasma scenario, and we enlarge the parametric space investigated. We then make use of the great advantage of METIS integrated simulations: we can evaluate not only the beam-plasma interaction (with a model accuracy similar to PENCIL), but also the response of the plasma itself (e.g. kinetic profiles) to NBI.

The injection line geometry was varied through the tangency radius and vertical tilt parameters. NBI power is fixed to 50 MW. We selected for the scan 16 tangency radii (corresponding to $R_{tang}$ = 6.68 : 10.71 m), 11 vertical tilts ($z_{ext}$ = 0 : 0.5) and 4 energies (500, 800, 1000, 2000 keV) for a total of 704 METIS simulations, resulting in the grid shown in fig. 4. Each grid point represents a possible injection geometry defined by its tangency radius and vertical tilt, at a given energy.

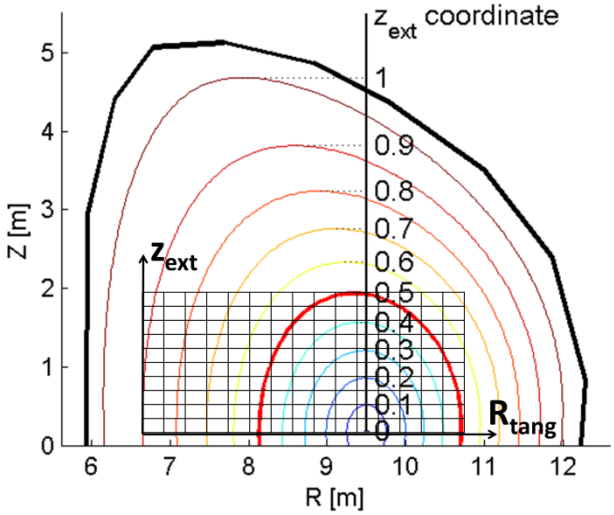


Figure 4: Grid representing the beam geometry options analysed in the METIS sensitivity study, superimposed on DEMO plasma equilibrium. Each grid point represents a possible injection line defined by its tangency radius ($R_{tang}$, in [m]) and vertical tilt ($z_{ext}$ [a.u.]), as defined in fig. 1.

As anticipated in [34] for 800 keV case, NBI shine-through during DEMO1 flat-top results to be not an issue, even at higher injection energy or very off-axis lines. This is shown in fig. 5 through a contour plot of shine-through losses in the $R_{tang}$-$z_{ext}$ plane for different energies. In all the cases analysed, the losses are well below 1% (i.e. < 0.5 MW) and increase slightly when moving the injection line off-axis. Similarly, first orbit losses are found low as well, around a few percent.

Fig. 6 shows the impact of different beam injection geometries and energies on plasma central electron temperature, $T_{e,0}$. We show $T_{e,0}$ since it a proxy on "how well" NBI is heating core plasma (DEMO1 requirement). Moreover, core plasma temperature affects strongly the total fusion power, which thus follows the behaviour of $T_e$. The parameter space around the reference DEMO NBI system described in section 2.3 ($R_{tang}$ = 7.09 m, no vertical tilt i.e. $z_{ext}$ = 0) corresponds to highest $T_{e,0}$, confirming the rationale of this choice. The increase of beam energy causes relatively small changes in plasma temperature: recall that $P_{NBI}$ = 50 MW compared to $P_{fus,alpha}$ ~ 400 MW, i.e. the real actuator of DEMO1 flat-top scenario is the heating from fusion alphas, not the auxiliary heating. Moving the injection line off-axis (horizontally or vertically) has a more significant effect. This is due to two, interdependent reasons. First, NBI is no longer heating the core plasma. Second, heating due to fusion is lowered due to the slight temperature reduction, and the decreased alpha heating in turn lowers the plasma temperature until a new balance is found. Fusion power reduction follows a similar trend of $T_{e,0}$, with a maximum reduction of ~15% for the most off-axis lines. The only reason to go to off-axis NBI injection would be to increase the current drive efficiency, e.g. to sustain advanced plasma scenarios with reversed safety factor profiles.

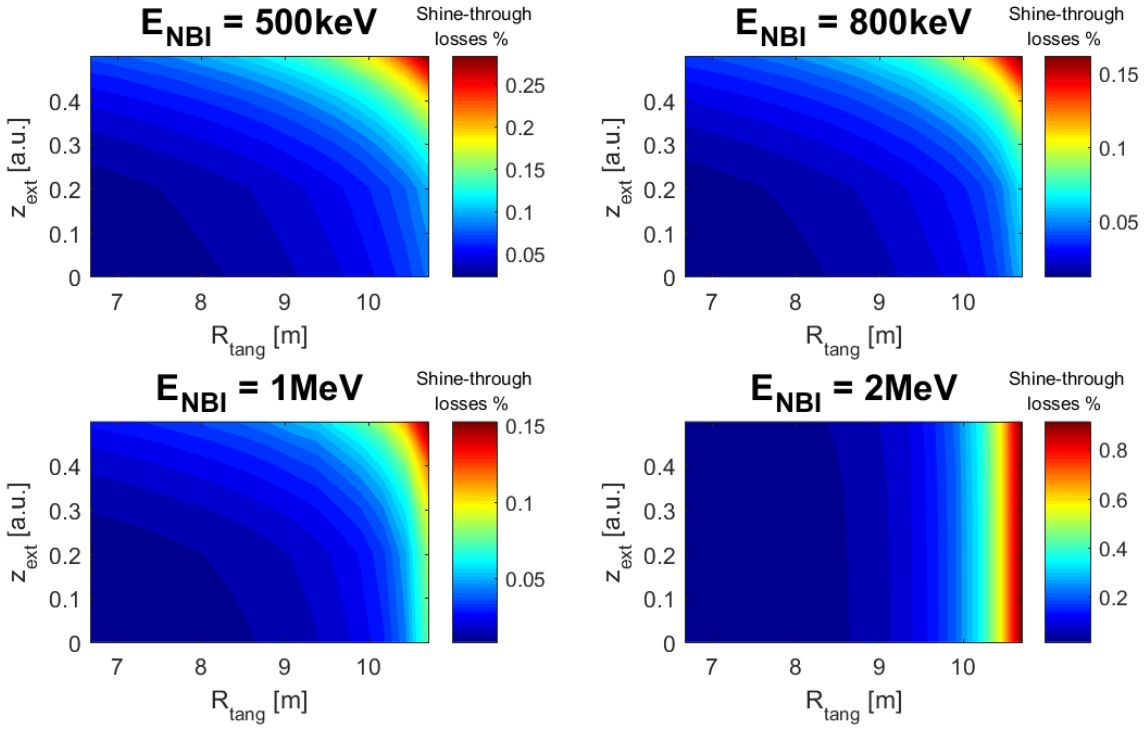


Figure 5: NBI shine-through losses estimated for different injection geometries in ($R_{tang}$, $z_{ext}$) space and energies, by METIS code. Different colour-scales, from blue (lowest % of shine-through losses) to red (highest), are indicated in the legend for each plot.

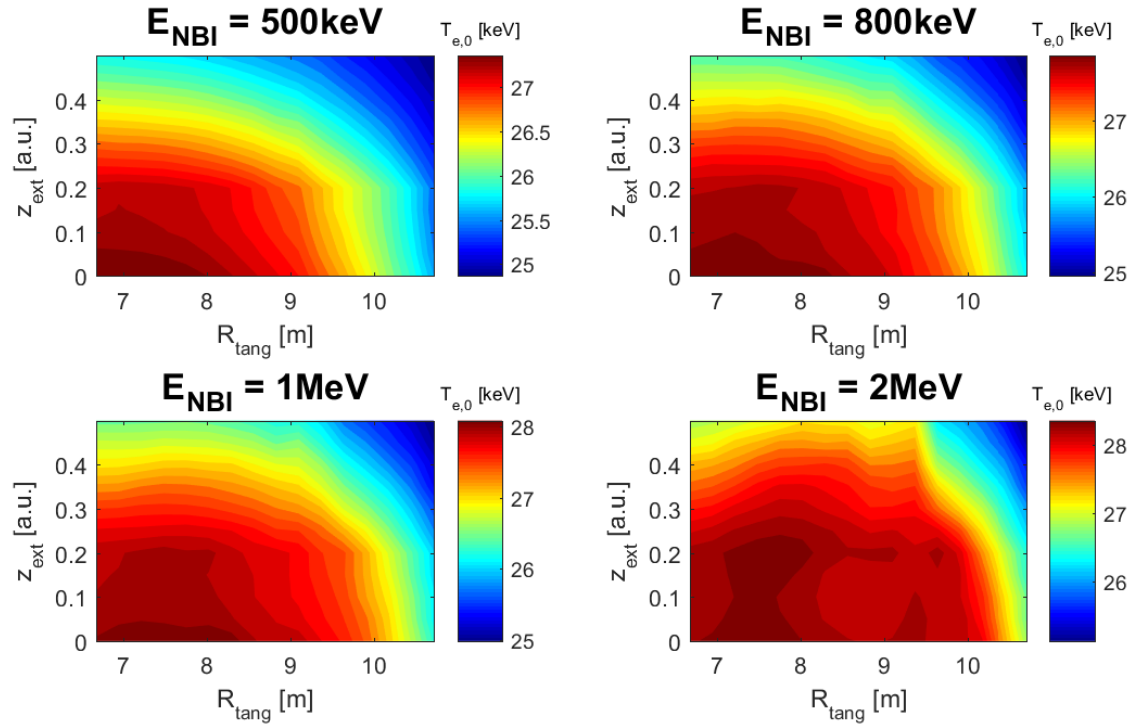


Figure 6: Central plasma electron temperature $T_{e,0}$ for different injection geometries in ($R_{tang}$, $z_{ext}$) space and energies, by METIS code. Different colour-scales, from blue (lowest $T_{e,0}$) to red (highest), are indicated in the legend for each plot.

We compared also the reference DEMO NBI with an identical injector but counter-current. Beside driving current in the opposite direction of the inductive plasma current, the main difference is the amount of fast ion losses, increased by a factor

of ~ 5. For completeness, also normal injection was simulated, showing obviously no current drive and no torque injection and a significantly increased amount of shine-through losses up to ~10% ($E_{NBI}$ = 800 keV, no vertical tilt), due to the shorter path in the plasma ending to the inner wall.

Clearly the whole parameter space shown in figures 5 and 6 is not accessible in reality, due to many engineering constraints and machine integration issues. Fewer selected cases, but feasible from the point of view of machine integration, are analysed more in details with ASCOT code in the next section.

### *4.2 Monte-Carlo ASCOT simulations of selected injection options*

Detailed simulations of beam-plasma interaction were carried out with Monte Carlo codes: BBNBI, for neutral beam ionization, and ASCOT, for fast ion slowing down. The aim of this section is to include in our analysis the engineering constraints which lead to a machine-integrated NBI system design. The reference injector is the one proposed in [23] and presented in section 2.3. Starting from this, we varied injection parameters to discuss the optimization from beam-plasma point of view.

Two possible horizontal injection angles were discussed from an engineering point of view in [23], i.e. 34.5° and 30° (ref.) at the intersection of the beam line and the first wall, also called “option 1” and “option 2” respectively. Both injectors have horizontal and vertical beam focuses at the wall port. The choice of the angle affects not only the beam absorption but also its integration with the machine, the impact on breeding blanket segments and the resulting tritium breeding ratio. “Option 2” became the reference option (as describe in sec. 2.3), due to its lower interference with breeding blanket segments. Another design (“option 3” in the paper [23]) was also proposed, with same injection angle as option 1, but with different port size: clearly this has no impact on beam-plasma interaction and is not considered in this paper. Together with “option 1” and “option 2” injectors, we included in the analyses also another injector, which we named “option 4”, with the beam focus (both horizontal and vertical) at the tangency radius, as it is for ITER, and injection angle of 30° at the first wall. This “option 4” was never considered from an engineering point of view, since it would require a much larger port size, but it is used here to compare the effect of different beam focuses. These three injector geometries (option 1, 2 and 4) were therefore implemented in BBNBI, which calculated the fast ion birth positions during plasma flat-top for $E_{NBI}$ = 800 keV, as illustrated in fig. 7, where the corresponding tangency radii of the options are reported too. Shine-through results in a few W for all the options, i.e. ~ 0 % of the injected power, in agreement with METIS results shown in section 4.1. The injection angles tested prevent the collision of the beam particles with the inner wall. The beam path is long enough to provide a complete beam ionization at the considered flat-top plasma density. The population of newly born fast ions was then evolved by ASCOT, giving as output the power deposition, driven current, torque and fast ion losses. Power density due to fast ion energy transfer is shown in fig. 8, where the three simulated options are compared (one injector each, injected power $P_{NBI}$ = 16.8 MW). All three injectors show centrally peaked profiles, with more accentuated differences between the two injection angles (“op. 1” vs “op. 2”) than between the two focuses (“op. 2” vs “op. 4”). The three injectors satisfy the DEMO1 requirement of core heating. Negligible fast ion orbit losses resulted for all the options. Table 3 summarizes the main results of the comparison. The driven current represent ~ 5 % of the total plasma current (note that values of table 3 have to be multiplied by 3 for the total current, as the number of DEMO injectors), but the injectors are not optimized for this purpose and current-drive efficiency can be further increased. Table 3 also highlights how moving the beam focus from the wall port to the plasma core has a negligible effect on beam-plasma interaction. This fact leaves some freedom of choosing the best beam focus to better cope with machine integration issues.

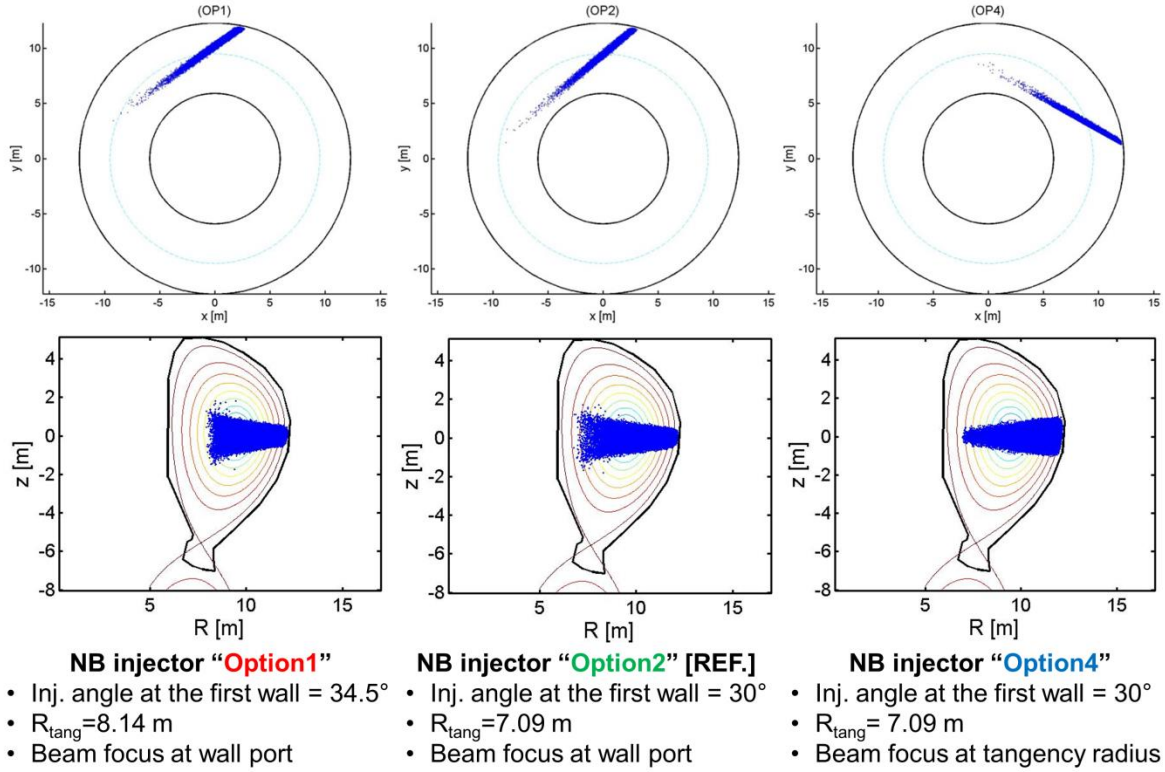


Figure 7: Horizontal (top) and poloidal (bottom) projection of neutral beam ionization points for one injector with three different injection geometries. "Option 4" is positioned at a different toroidal angle, but, except for the beam focus, is identical to "Option 2". Injection is on the mid-plane at $E_{NBI}$ = 800 keV and $P_{NBI}$ = 16.8 MW. Flat-top plasma is described in table 1 and fig. 2.

| Simulations with one injector only $P_{NBI}$ = 16.8 MW | **Op. 1 34.5°** | **Op. 2 30°** | **Op. 4 pl. focus** |
|---|---|---|---|
| **Coupled power to plasma %** | 99.7 | 99.7 | 99.7 |
| **Shine-through losses %** | 0.0 | 0.0 | 0.0 |
| **Fast ion orbit losses %** | 0.3 | 0.3 | 0.3 |
| **Driven current [MA]** | 0.5 | 0.3 | 0.3 |
| **Torque [N m]** | 29.0 | 25.2 | 25.2 |

Table 3: Summary of ASCOT simulations for three different neutral beam injection geometries, at $E_{NBI}$ = 800 keV and $P_{NBI}$ = 16.8 MW. Flat-top plasma is described in table 1 and fig. 2.

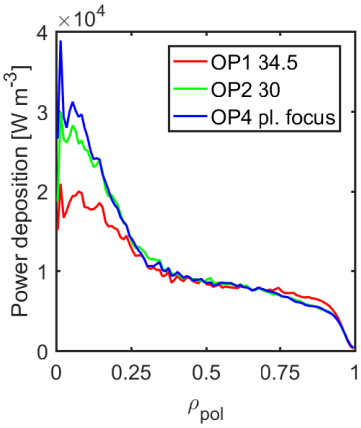


Figure 8: NBI power deposition for three different injector options of fig. 7.

After exploring different injection geometries, we concentrated on the analysis of "option 2" geometry ($R_{tang}$ = 7.09 m), being the chosen reference design in [23] and [34]. From now on, simulations, figures and tables refers to the complete DEMO NBI system, i.e. formed by three injectors with a total power of $P_{NBI,tot}$ = 50.4 MW and geometry as "option 2", unless told otherwise. Fig. 9 shows the density of newly-born fast ions on horizontal and poloidal planes for different $E_{NBI}$ values. The beamlet geometry is not changed in the following simulations, although changing $E_{NBI}$ at constant $P_{NBI}$ would require reassessing the beam extracted current and optics properties. The focus here is indeed to investigate the sensitivity to beam energy only. As the beam energy is increased from 500 keV to 2 MeV, the path of the beam inside the plasma become longer. We can also observe that the 500 keV option has the highest edge fast ion density. There are two reasons for this. First, at lower energy and fixed power, the number of injected particles is higher. Second, at low energy, the ionization mean-free-path is shorter.

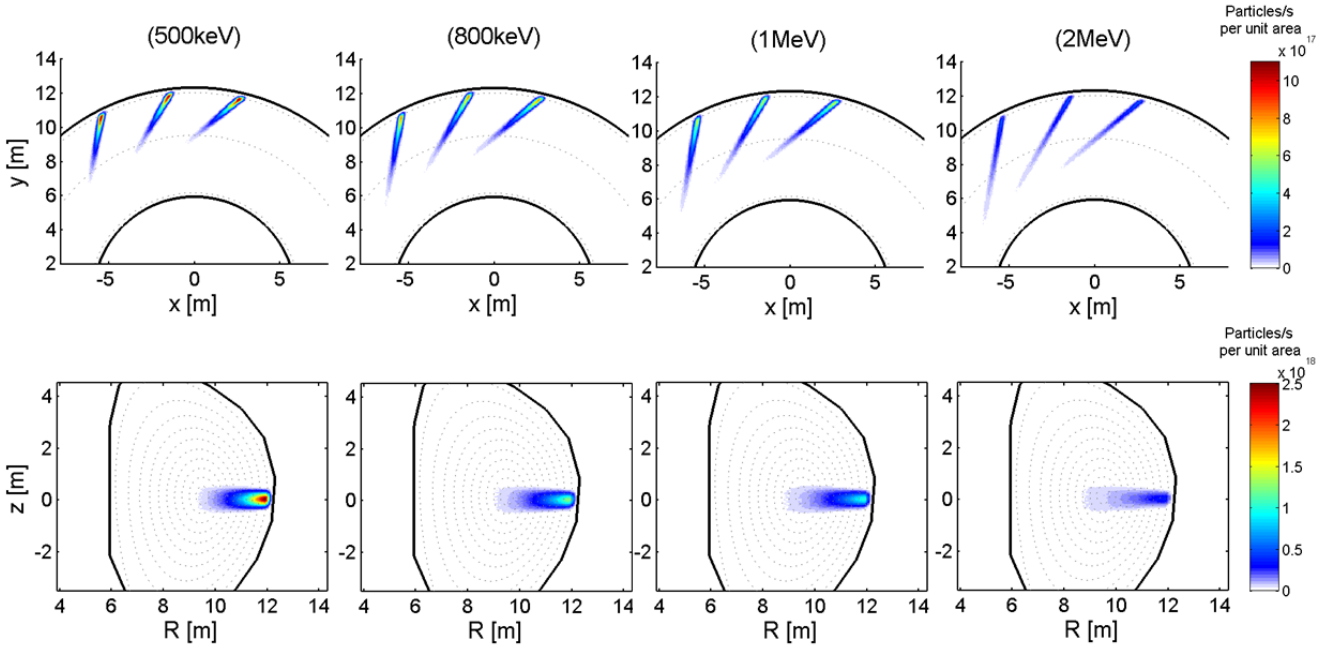


Figure 9: Beam ion source (particle/s) on horizontal (top) and poloidal (bottom) planes, at different injection energies ($E_{NBI}$ = 0.5, 0.8, 1, 2 MeV) for three injectors ($P_{NBI,tot}$ = 50.4 MW) with geometry as "option 2", during DEMO1 flat-top.

Significant edge ionization of 500 keV injector is also evident in the radial profile in fig. 10a. Fast ion birth density profiles (fig. 10a) are generally peaked in the centre, due to the small volumes of central plasma region.

Fig. 10b shows the radial profile of power deposition to the plasma, which, for all the energies analysed, is centrally-peaked. 500 keV option has the lowest difference between central and peripheral power deposition, while higher energies have power depositions strongly peaked in the core. For DEMO1 requirement of core plasma heating, beam energies $\gtrsim$ 800 keV are thus recommended.

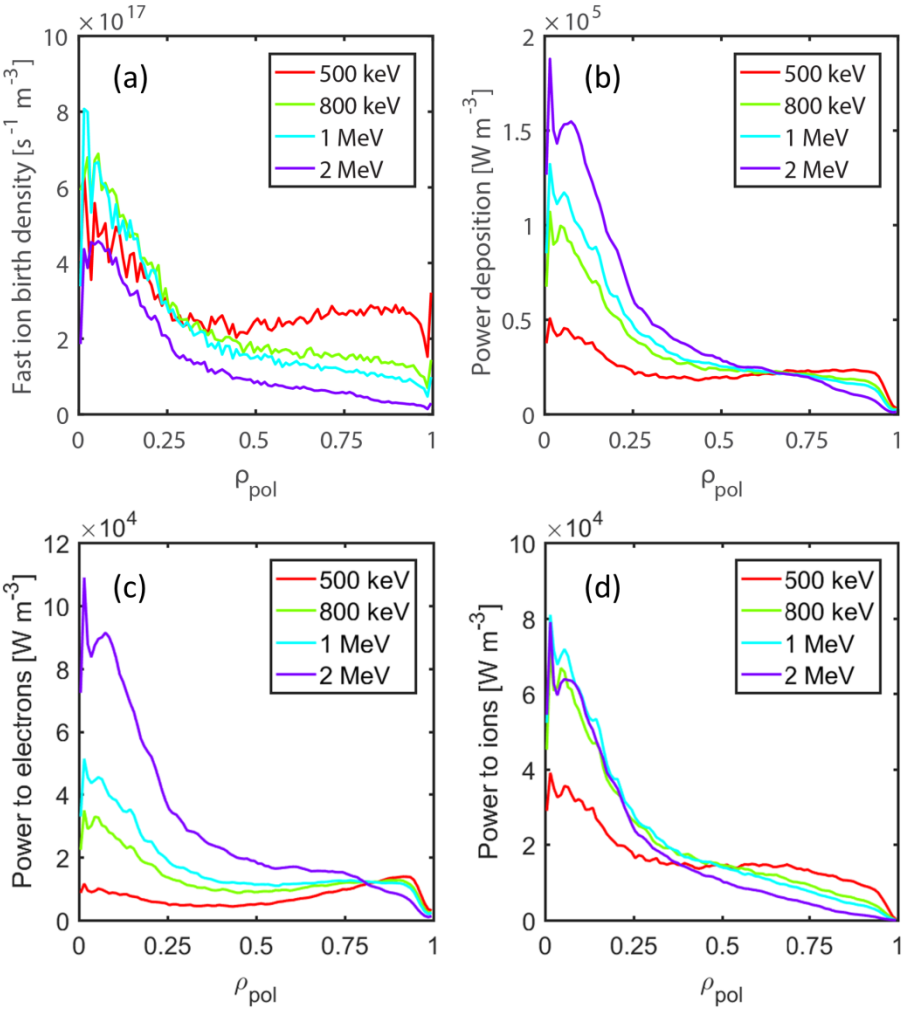


Figure 10: Radial profiles of beam-ion birth density (a), total power deposition to the plasma (b), power deposition to electrons (c) and power deposition to ions (d) for different beam energies.

Figures 10c and 10d illustrate the power deposition profiles separately to electrons and ions. If we compare the same injection energy, the power is deposited more to electrons in the edge and more the ions in the core, due to the aforementioned $T_e$ dependence of the local critical energy $E_c$ (defined in sec. 3).

Fig. 11a shows the driven current profiles which are centrally peaked, thus sustaining the inductive plasma current. Fig. 11b depicts the NBI input torque to the plasma. The NBI torque density to the plasma peaks at the magnetic axis for all the cases. A summary of the energy scan is reported in table 4 with the values of fast particle losses, volume-integrated driven current, torque and particle source.

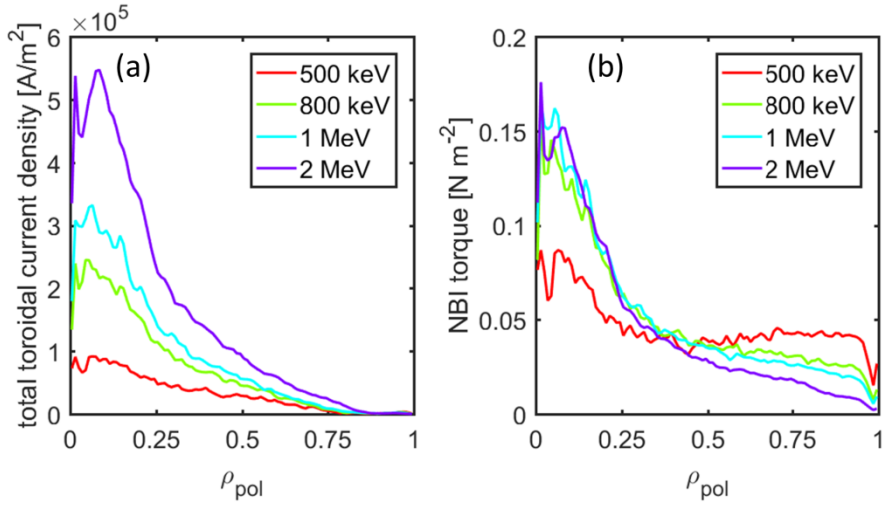


Figure 11: Radial profiles of driven current density (a) and input torque to the plasma (b) for different beam energies.

The volume-integrated NBI power transferred to plasma electrons increases with the injection energy, as depicted fig. 12a. At 800 keV, the power is almost equally deposited to ions and electrons, slightly in favour of the electrons. The power coupled to the plasma is, in all cases, almost the entire injected power, with losses accounting for less than 0.6%. Shine-through is almost zero, while for lower energy beams we have slightly higher orbit losses. This is due to the more peripheral ionization of low energy beams.

| Simulations with three injectors $P_{NBI}$ = 50.4 MW | **500 keV** | **800 keV** | **1 MeV** | **2 MeV** |
|---|---|---|---|---|
| **Coupled power to plasma %** | 99.4 | 99.7 | 99.7 | 99.9 |
| **Power to ions %** | 56.4 | 48.8 | 44.8 | 31.3 |
| **Power to electrons %** | 43.6 | 51.2 | 55.2 | 68.7 |
| **Shine-through losses %** | 0.0 | 0.0 | 0.0 | 0.1 |
| **Fast ion orbit losses %** | 0.6 | 0.3 | 0.4 | 0.0 |
| **Driven current [MA]** | 0.6 | 1.0 | 1.3 | 2.1 |
| **Torque [N m]** | 94.9 | 75.9 | 68.2 | 48.9 |
| **Fuelling [$10^{20}$ part/s]** | 6.3 | 3.9 | 3.2 | 1.6 |

Table 4: Summary of ASCOT simulations of different neutral beam injection energies. Plasma parameters are described in table 1.

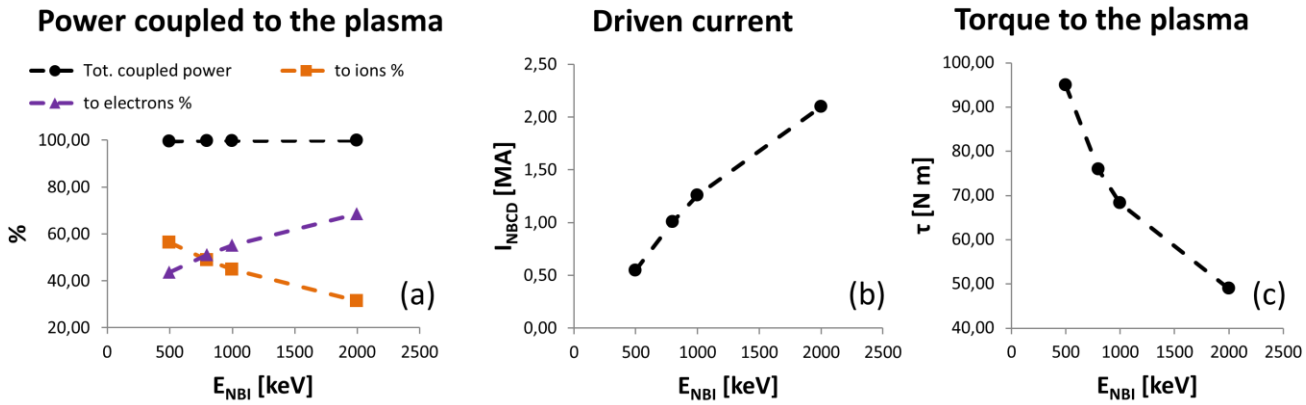


Figure 12: Trends of NBI coupled power to plasma - total, ions and electrons - (a), driven current (b) and torque to the plasma (c) for different neutral beam injection energies.

Current drive increases almost linearly with energy (fig. 12b). The corresponding current drive efficiency [$10^{20}$ A · $W^{-1}$ · $m^{-2}$] varies from $\eta_{NBCD}$ = 0.08 at 500 keV to 0.30 at 2 MeV. An optimized NBI system with appropriate injection line for current drive may reach even higher $\eta_{NBCD}$ values, suitable to sustain advanced, steady-state DEMO scenarios. NBI torque (fig. 12c) decreases with $E_{NBI}$ due to the lower momentum transfer to ions: DEMO plasma rotation is expected anyway to be low due to the high plasma inertia.

Keeping $P_{NBI}$ fixed, different beam energy implies different fuelling, defined as the number of ionized particles in the plasma per second, having highest fuelling at lowest energy (see table 4) due to largest number of particle injected ($\propto {P_{NBI}}/{E_{NBI}}$). If compared to other particle sources [42], NBI at ~1 MeV anyway provide less than 1% of fuelling, being therefore a negligible particle source due to the large plasma volume and the magnitude of the injected power. In [42], although with a prior DEMO design, it was shown that NBI does not significantly unbalance the 50:50 D:T mixture of DEMO even locally. Therefore tritium NBI is not needed, simplifying the design of DEMO injectors.

The slowing-down distribution function for $E_{NBI}$ = 800 keV is depicted in fig. 13a versus the radial coordinates $\rho_{pol}$, together with the profile of the critical energy $E_c$. The highest populated region is ~200:400 keV in core plasma (fig. 13a, at $\rho_{pol}$~0), where $E_c$ has its maximum, $E_c$ > 400 keV: this is indeed the region with more ion heating. The strong presence of slowing down beam ions in the plasma core instead of plasma edge, where $E_c$ is lower than its volume-averaged value, makes the final fraction of power going to ions a bit larger than supposed through basic considerations in section 3. In fig. 13b we can observe the volume-integrated fast ion slowing-down density as function of fast ion energy. Note that fast ions injected at 800 keV are not only slowed down, but in minority also scattered to higher energies due to Coulomb collisions.

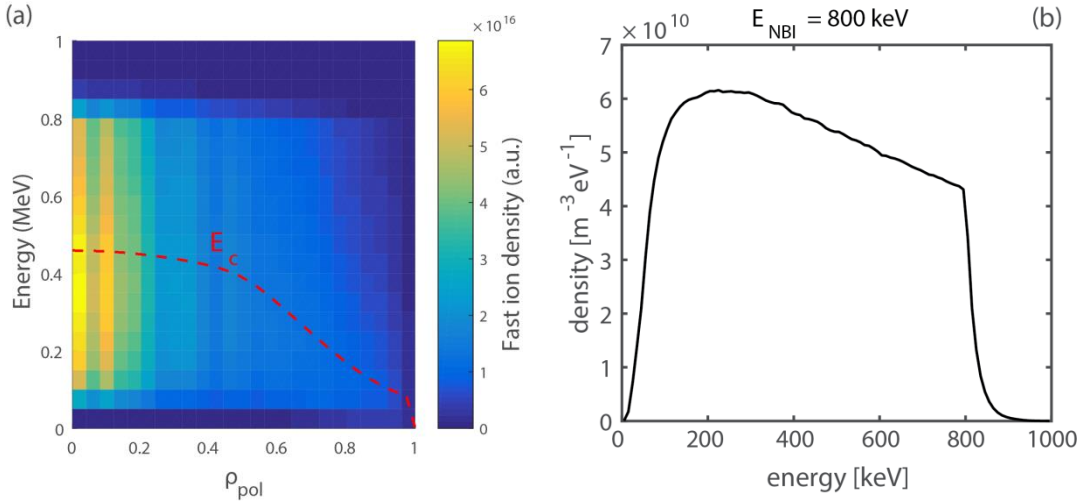


Figure 13: Slowing-down distribution functions ($E_{NBI}$ = 800 keV, $P_{NBI,tot}$ = 50.4 MW): a 2D distribution in ($\rho_{pol}$, energy) space (a) and volume-integrated fast ion density versus energy in (b). Critical energy $E_c$ profile is superimposed in red in (a).

A scan in impurity content, through effective charge values of $Z_{eff}$ = 1.4, 1.8, 2.2, 2.6, was also carried out with ASCOT, keeping the same mix of impurities but increasing their concentrations. Only limited effects are noted, with an increase of ~10% of driven current from $Z_{eff}$ = 1.4 to 2.6. The beam ionization is already very efficient in the reference case, with no shine-through losses, and fast ion birth profiles are very similar when varying the effective charge within the chosen range. Therefore, for DEMO1 flat-top, a limited $Z_{eff}$ variation in the plasma is not affecting significantly beam-plasma interaction.

## 5. NBI operation during transient phases: the ramp-up case

While H&CD power needs during flat-top phase have been widely discussed, it is now clear that auxiliary power is essential also during DEMO transient phases [5]. For instance, during current ramp-up, the plasma needs auxiliary power to warm up, access the H-mode, and enter the fusion power dominated flat-top phase. Since usually the H&CD systems are optimized to work for plasma flat-top parameters, it is essential to evaluate their operability and performance also during the transient phases, where their contribution is critical. A first discussion on heating systems during transient phases was presented in [5], while in [43] NBI operation during DEMO ramp-up was investigated in details for $E_{NBI}$ = 800 keV. Here we review the operational window of NBI during ramp-up, including in the study also other beam energies than 800 keV (i.e. 500 keV, 1 and 2 MeV). For sake of clarity, the different options are compared keeping the same beamlet geometry and injected power. We also propose a formula that fits the fraction of shine-through losses for DEMO NBI at low densities in section 5.1.

A crucial parameter to decide when NBI can be switched-on during ramp-up is the maximum tolerable heat flux on the DEMO1 first wall. In fact, the tolerable heat flux due to NBI on the first wall for DEMO has not yet been fixed. The maximum power load assumed for DEMO1 flat-top in static conditions is 1 MW/m$^2$ [44], which includes all the possible heat fluxes, not only from NBI but also radiation, charged particles, ELMs etc. . Considering an axisymmetric magnetic field, shine-through losses represents the only localized beam loss that could significantly harm the first wall. During ramp-up, most of these heat fluxes on the wall are reduced or absent, but NBI shine-through can be considerable. In the ITER case, the maximum allowed power load due to NBI shine-through during ramp-up is $P_{NBI,shine}$<0.5 MW/m$^2$ [45]. If a first wall armour is installed, $P_{NBI,shine}$ for ITER could be increased up to ~ 4 MW/m$^2$. To limit the peak shine-through power on the first wall, there are different options: avoid using NBI until higher plasma densities are reached, decrease the injected NBI power, or lower the injection energy. A modular injector, as the one presented in [23], is capable of operating at reduced power, either switching off some of the modular sources or at reduced energy decreasing the accelerating voltage. Consequently, the available NBI power results $P_{NBI} \lesssim P_{NBI,max} \cdot \frac{E_{NBI}}{E_{NBI,max}}$. These capabilities already allow the use of NBI during transient phases even with inefficient beam ionization.

Fig. 14 shows the shine-through footprint on DEMO first wall for one injector at full power ($P_{NBI}$ = 16.8 MW) at 1 MeV energy, with the injection geometry described in section 2.3. The ramp-up plasma profiles are those shown in fig. 3. The peak heat flux becomes less intense during ramp-up, as the plasma density increase. The “thin and tall” beam shape is recognisable. The highest power load is in the central region of the footprint, where the majority of the beamlets are focused.

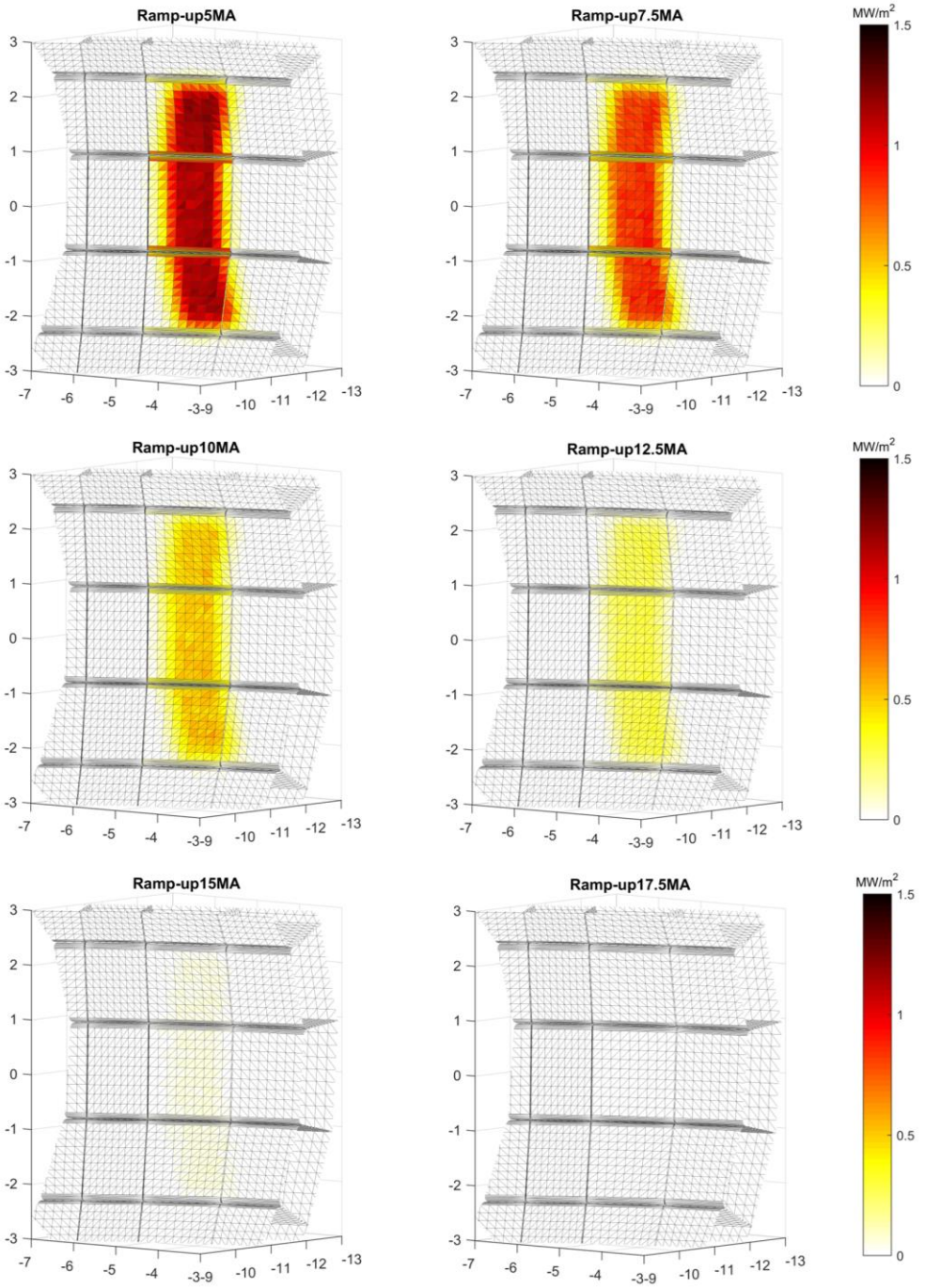


Figure 14: Power density on DEMO1 first wall ("footprint") due to NBI shine-through losses (1 injector, $P_{NBI}$ = 16.8 MW, $E_{NBI}$ = 1MeV, injection geometry as in table 2) during the ramp-up phase illustrated in fig. 3. Losses increases from white to black.

Table 5 summarizes all the simulated cases for DEMO1 ramp-up. Increasing the injection energy makes the shine-through losses increase as expected. The maximum shine-through is reached at the lowest analysed density for 2 MeV case (> 50 % of the injected power). Fast ion orbit losses are always low, in the order of 1 %. In case of different injected power but equal plasma kinetic profiles, the ratio of coupled power to plasma and fast particle losses remain unchanged, while current drive and peak shine-through scale linear with the injected power. Fig. 15 shows the shine-through losses at different ramp-up densities for the simulated injection energies. Shine-through loss fraction has an exponential dependence on plasma density, due to the $1/n$ dependence of the beam mean free path. If we use the ITER limit for NBI shine-through ($P_{NBI,shine}$<0.5 MW/m$^2$), we can safely start NBI at full power (16.8 MW per injector) at $\langle n_e \rangle_{min}$ = 1.01, 1.36, 1.78 and 2.92 · $10^{19}$ m$^{-3}$ for

$E_{NBI}$ = 500 keV, 800 keV, 1 MeV and 2 MeV respectively. For comparison, ITER minimum density for NBI switch-on (for Hydrogen operations) is $\langle n_e \rangle_{min} \sim 3 \cdot 10^{19}$ $m^{-3}$. A more favourable condition for NBI during ramp-up is therefore found for DEMO with respect to ITER, for all the analysed beam energies. In addition, NBI energy and power modulation can further enlarge the NBI ramp-up operability.

Note that, in the early ramp-up phase, NBI shows a very high current drive efficiency, which is then reduced when approaching the flat-top phase. This is due to the fact that the current drive efficiency depends on the ratio $E_{NBI}/E_c$: this ratio has its maximum at low temperature in the beginning of ramp-up and then decreases. Consequently, the NBI driven current decreases as well. An efficient current drive in the early ramp-up phases, seen for all the analysed energies, can help in saving central solenoid flux.

A figure of merit, not to be ignored for ramp-up phase, is the physics governing the L-H transition. In general, L-H transition can be triggered also during the flat-top phase, depending on the strategy adopted. In the last years, the role of the ion heat channel has been highlighted as the relevant parameter for L-H transition [46]. Ion heating can be provided by direct auxiliary heating (e.g. RF antennas or NBI) and by electron-ion heat exchange, depending on plasma collisionality. According to this recent L-H theory, in case of direct electron heating (e.g. ECRH), part of the power necessary to reach the L-H power threshold "$P_{L-H}$" is dispersed, not reaching the ion channel, causing an increase in the auxiliary power needed for L-H access. At ASDEX-Upgrade [46], it was demonstrated that with NBI alone, which heats mainly ions at that energy, $P_{L-H}$ was 40% lower than with ECRH. Adding ECRH made $P_{L-H}$ increase by the amount of ECRH added, showing that additional ECRH power did not contribute to the access to H-mode, being the ion heat flux dominated by NBI. The role of the ion heat channel was confirmed in other tokamaks (e.g. Alcator C-mod [47]), while it is being discussed for JET [48]. In addition, an effective ion heating during the ramp-up phase would bring D and T ions in the fusion temperature range, so that alpha heating can help to reach the stationary fusion-dominated conditions. For DEMO, NBI heats both ions and electrons, but still the ion heating is considerable, ~50% at 800 keV in flat-top condition (sec. 4.2). DEMO density being higher than that in present-day devices, one can expect collisional energy exchange to be more efficient in transferring the power from electron to ion channel, easing the triggering of L-H transition. However, the L-H transition plasma density for DEMO is not known. At the beginning of the ramp-up here analysed, for all injection energies, the majority of the power is transferred to electrons, which reaches its maximum for $E_{NBI}$ = 2 MeV at density $\langle n_e \rangle$ = 0.78 $10^{19}$ $m^{-3}$: 85.57 %. The fraction of NBI power to the ions is however significant (~ 30 - 40%) for 800 keV and 1 MeV cases during the whole ramp-up, and increases as the plasma temperature increases. Since both the partition of the deposited power and the current driven by NBI depend on the electron temperature (via the critical energy and resistivity, respectively), they will be strongly influenced by the adopted ramp-up strategy.

| | **Ramp-up snapshots** | | | | | | |
|---|---|---|---|---|---|---|---|
| ***Plasma*** | | | | | | | |
| ***$\langle n_e \rangle$ [$10^{19}$ $m^{-3}$]*** | *0,78* | *1,01* | *1,36* | *1,78* | *2,92* | *5,11* | *6,54* |
| ***Ip [MA]*** | *5,0* | *7,5* | *10,0* | *12,5* | *15,0* | *17,5* | *19,6* |
| ***$\langle T_e \rangle$ [keV]*** | *5,92* | *5,50* | *5,73* | *5,95* | *6,22* | *8,19* | *12,89* |
| ***Plasma volume [$m^3$]*** | *1843* | *2012* | *2086* | *2202* | *2313* | *2384* | *2434* |
| **$E_{NBI}$ = 500 keV** | | | | | | | |
| **shine-through %** | 17,2 | 10,3 | 4,5 | 1,7 | 0,1 | 0,0 | 0,0 |
| **peak shine-through wall load [MW/$m^2$]** | 0,7 | 0,4 | 0,2 | 0,1 | 0,0 | 0,0 | 0,0 |
| **fast ion orbit losses %** | 0,6 | 0,9 | 0,4 | 0,5 | 1,8 | 1,1 | 1,6 |
| **power to ions %** | 42,6 | 50,9 | 53,2 | 52,0 | 47,9 | 48,2 | 57,8 |
| **power to electrons %** | 57,4 | 49,1 | 46,8 | 48,0 | 52,1 | 51,9 | 42,2 |
| **driven current [MA]** | 10,7 | 10,4 | 7,4 | 5,5 | 2,8 | 1,0 | 0,8 |
| **$E_{NBI}$ = 800 keV** | | | | | | | |
| **shine-through %** | 28,6 | 19,9 | 10,9 | 5,4 | 0,8 | 0,0 | 0,0 |
| **peak shine-through wall load [MW/$m^2$]** | 1,1 | 0,7 | 0,4 | 0,2 | 0,1 | 0,0 | 0,0 |
| **fast ion orbit losses %** | 1,0 | 1,0 | 0,5 | 0,4 | 0,9 | 0,5 | 0,9 |
| **power to ions %** | 31,8 | 39,5 | 41,8 | 41,2 | 39,2 | 39,4 | 48,9 |

| | | | | | | | |
|---|---|---|---|---|---|---|---|
| **power to electrons %** | 68,2 | 60,5 | 58,2 | 58,8 | 60,8 | 60,6 | 51,1 |
| **driven current [MA]** | 10,5 | 11,0 | 8,5 | 6,7 | 3,7 | 1,6 | 1,4 |
| **$E_{NBI}$ = 1000 keV** | | | | | | | |
| **shine-through %** | 34,6 | 25,4 | 15,3 | 8,4 | 1,6 | 0,0 | 0,0 |
| **peak shine-through wall load [MW/m$^2$]** | 1,2 | 0,9 | 0,6 | 0,3 | 0,1 | 0,0 | 0,0 |
| **fast ion orbit losses %** | 1,0 | 0,9 | 0,5 | 0,4 | 0,8 | 0,4 | 0,6 |
| **power to ions %** | 27,1 | 34,7 | 36,6 | 36,1 | 34,5 | 35,0 | 44,5 |
| **power to electrons %** | 72,9 | 65,3 | 63,4 | 63,9 | 65,5 | 65,0 | 55,5 |
| **driven current [MA]** | 9,7 | 10,9 | 8,6 | 6,9 | 4,0 | 1,8 | 1,7 |
| **$E_{NBI}$ = 2000 keV** | | | | | | | |
| **shine-through %** | 54,3 | 44,5 | 32,9 | 23,1 | 8,6 | 1,1 | 0,3 |
| **peak shine-through wall load [MW/m$^2$]** | 2,1 | 1,6 | 1,2 | 0,9 | 0,3 | 0,1 | 0,0 |
| **fast ion orbit losses %** | 1,5 | 0,9 | 0,4 | 0,4 | 0,8 | 0,3 | 0,3 |
| **power to ions %** | 14,4 | 18,7 | 22,5 | 22,3 | 21,9 | 22,3 | 30,6 |
| **power to electrons %** | 85,6 | 81,3 | 77,5 | 77,7 | 78,1 | 77,7 | 69,4 |
| **driven current [MA]** | 6,6 | 7,7 | 7,4 | 6,4 | 4,6 | 2,4 | 2,7 |

Table 5: Summary of ASCOT simulations of different neutral beam injection energies during different stages of DEMO ramp-up phase, illustrated in fig. 3. The peak shine-through wall load is referred to a single injector, while the driven current takes into account three injectors ($P_{NBI,tot}$ = 50.4 MW, $P_{NBI,\ single\ injector}$ = 16.8 MW).

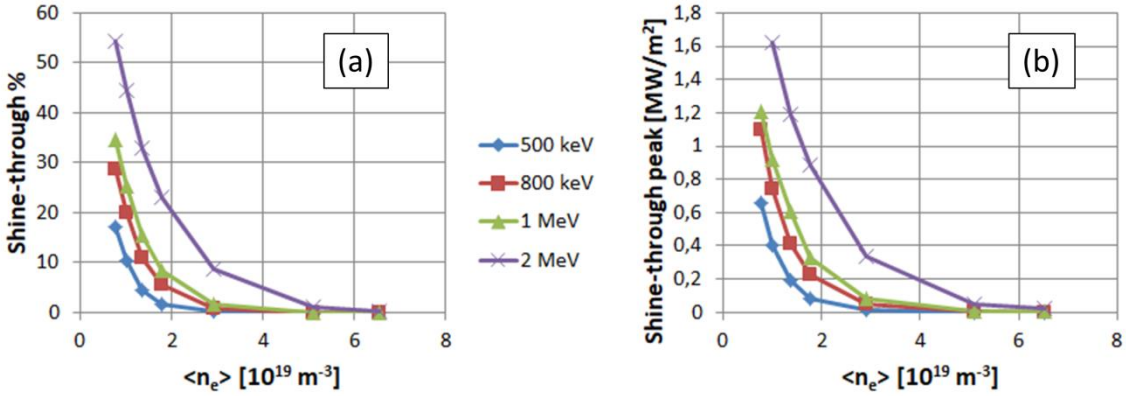


Figure 15: NBI shine-through losses in percentage (a), and consequent peak power [MW/m$^2$] to the first wall (one injector, $P_{NBI}$ = 16.8 MW) versus volume-averaged plasma electron density, for different injection energies.

The analysis presented in this section is valid not only for the ramp-up phase, but for any DEMO plasma which exhibits similar densities. Therefore any unforeseen transient with reduced plasma density during flat-top phase, or the ramp-down phase, can be described by similar beam-plasma physics. From the point of view of NBI, the largest difference between ramp-up and ramp-down is the amount of power required, which depends, for instance, on the plasma radiation that has to be balanced, and on the magnitude of fusion alpha heating. We leave the development of DEMO transient phase strategy to future studies.

### *5.1 Multi-variable regression of DEMO shine-through fraction*

In order to extend the usability of this study to other DEMO cases, we exploited the BBNBI energy/density scan carried out in the previous section to perform a multi-variable regression of the shine-through fraction, as a function of volume-averaged plasma density and beam energy. This approach is the same used for ASDEX-Upgrade (AUG) tokamak shine-through formula (reviewed and updated in [49]), exploiting the exponential decay of the neutral beam intensity in the plasma due to ionization. The fit is valid for machines of the size of DEMO and for similar tangential injection geometries, since it does not take into account any geometrical parameter. The resulting formula for shine-through fraction yields:

$$ST_{fraction} = e^{\left(-\frac{<n_e>^{1.049\pm3.5E-05} E_{NBI}^{-0.746\pm6.9E-05}}{0.0043\pm1.4E-05}\right)} \qquad \text{(eq. 1)}$$

with $<n_e>$ in $10^{19}$ $m^{-3}$ and $E_{NBI}$ in keV. The formula is obtained for deuterium NBI in D:T plasmas. The root mean square error of the regression is RMSE = 10.82%. This formula reproduces well the simulation results, as shown in fig. 16. As fitting parameter, we used the volume-averaged density, a parameter easily available for any DEMO plasma. In fact the relevant parameter would be the particle density that the neutral beam finds along its trajectory. Therefore eq. 1 is reliable for other DEMO-size plasmas if density peaking factor, i.e. density profile shape, does not change significantly (here, $n_{e,peaking}$ ~ 1.3) and the beam trajectory is not considerably different (i.e., not for normal injection cases). The dimension and shape of the beam inside the plasma should not significantly affect the regression due to the large DEMO volume: a different beam shape (e.g. circular instead of "thin and tall") should not modify much the number of particles encountered by the beam in the plasma. In principle, other parameters can be included in the regression (e.g. temperature or $Z_{eff}$), but we did not have enough cases to consider these variables as independent. Anyway, the exponents of the parameters in eq. 1 are close to what found for AUG, despite the differences in machine dimension, beam energy and injection geometry. This confirms that the most significant parameters for shine-through are only the electron plasma density and NBI energy. The peak shine-through wall load [$MW/m^2$] cannot be satisfactorily fitted by a power law or an exponential function of density and beam energy. However, the extrapolation of the peak shine-through wall load to other DEMO machines would be uncertain, since it depends on how the first wall is shaped (e.g. tiles, gaps…), and on the geometry of the NBI beamlets itself.

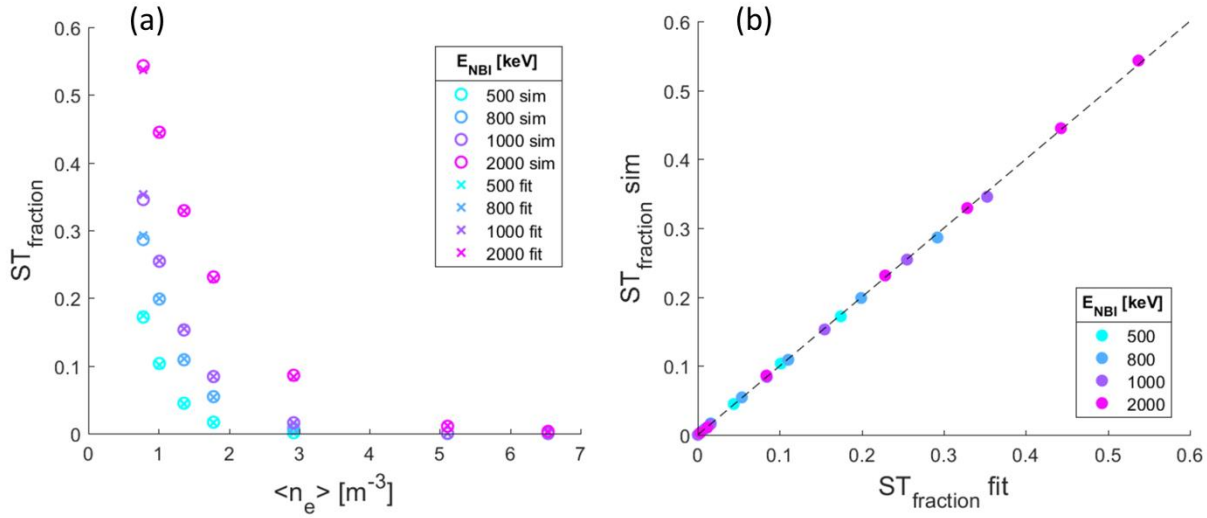


Figure 16: NBI shine-through loss fraction versus volume averaged electron density during DEMO1 ramp-up (simulated – circles - and fitted values with eq. 1- crosses) in (a) and a direct comparison between shine-through loss fraction estimated by BBNBI code and the fit in eq. 1 in (b).

## 6. Summary and conclusions

The DEMO heating mix is still not decided, and NBI is a candidate auxiliary power system, due to its reliability, effectiveness and long operational experience in fusion devices. An auxiliary power system for a DEMO1 pulsed plasma has to provide bulk heating during the stationary, flat-top phase and possibly sustain the plasma during the initial and final transient phases. The present integrated study discussed how an optimized NBI can fulfil these requirements, in an unprecedented parameter space with respect to current NBI systems and plasma volume, larger even than ITER.

This scope was achieved investigating the axisymmetric plasma response to NBI through wide-range sensitivity studies with METIS 0.5D transport code and through detailed modelling with ASCOT Monte Carlo code of different injector options based on realistic engineering designs. We analysed in particular the NBI design reported in [23], which describes an injector system optimized for DEMO in terms of overall system efficiency and machine integration, and compatible with different neutralizer technologies.

Co-current tangential injection is the preferred DEMO1 scheme, minimizing fast particle losses compared to perpendicular or counter-current injection. To minimize shine-through losses, it is essential to avoid a beam line that intersects the inner wall of the machine: the beam path in the plasma would be too short. The parameter space (injection geometry, energy) around

DEMO NBI parameters defined in [23] (specifically "Option 2" design, $R_{tang}$ = 7.09 m, no vertical tilt) presents the best solution for high fusion power, high core plasma temperature and negligible fast particle losses both at 800 keV and 1 MeV beam particle energy. Little variations on the injection angle (e.g. few degrees), or a different beam focus (e.g. at the wall port or at the tangency radius) do not affect significantly the beam power deposition. As a consequence, a beam line designed to be mechanically vertically-tilted of a few degrees during operations would not bring any clear advantage. Given the sensitivity scan results, we leave some freedom for the NBI system design to comply with the machine integration requirements, e.g. a minimum impact on breeding blanket modules or avoiding any interference with the magnetic field coils.
NBI having injection energy $E_{NBI} \gtrsim 800$ keV aimed tangentially at the plasma core fulfils the central heating requirement, for the DEMO1 plasma analysed. From the technological point of view, the extracted negative ion current request from the beam source, which is a delicate parameter, would be decreased in case of higher injection energy. On the other hand, the feasibility of systems with $E_{NBI} > 1$ MeV is still under discussion, due to the complicate voltage handling. Higher injection energy (e.g. 2 MeV) would increase the NBI driven current and energy transfer to electrons, still with negligible fast particle losses during flat-top phase. Anyway, NBI current drive is not specifically required for DEMO1 flat-top plasma.
The fuelling contribution from a deuterium NBI, with energy and power in the range of 800-1000 keV and ~50 MW, is negligible, and will not unbalance the D:T ratio in the plasma [42]. This implies that a more complex tritium NBI is not requested for DEMO. Small changes in impurity content ($1.4 < Z_{eff} < 2.6$) do not significantly affect beam-plasma interaction. The NBI operability window during transient phases was investigated, showing that this window is even larger than the ITER case. This is due to the larger DEMO plasma volume. The critical parameter is the allowed power load on the first wall due to shine-through losses, which at the moment is under definition for DEMO: for this study we used the value of ITER ($P_{NBI,shine}<0.5$ MW/m$^2$ [45]). Based on this criterion, we estimated the lowest density at which a given NBI system can be safely operated at full power, for different values of energy: $\langle n_e \rangle_{min} \sim 1.01, 1.36, 1.78$ and $2.92 \cdot 10^{19}$ m$^{-3}$ for $E_{NBI}$ = 500 keV, 800 keV, 1 MeV and 2 MeV respectively. In case of NBI system capability for power/energy modulation (as it is for the injector designed in [23]), the low-density operability of the system can be further extended if operated at lower power or energy. This highlights the importance of studying modular NBI systems for future reactors. A shine-through parametrization for DEMO-like machines was proposed in terms of volume-averaged electron density and beam energy (eq. 1). One of the main duties of auxiliary power during ramp-up/early flat-top phase is to enable the access to the H-mode. Recent studies [46] proposed the importance of the ion heat channel to trigger the L-H transition, and showed how, for ASDEX-Upgrade tokamak, direct electron heating (from ECRH power) did not directly contribute to the transition. In DEMO, plasma density is expected to be higher and, therefore, a more efficient electron-ion energy transfer should contribute to balance the ion heating. However, for each ramp-up stage analysed, we reported the beam direct ion heating, which was found in the range of 30-40% of the total power during the whole ramp-up for 800 keV and 1 MeV cases. Reducing the beam particle energy to 500 keV would result in more than 50% of beam power coupled to plasma ions, throughout most of the ramp-up phase analysed. Direct ion heating would be also beneficial to bring D and T ions to fusion-relevant temperatures, in order to accelerate the transition to the stationary phase dominated by alpha-particle heating. It is interesting to note the high current drive efficiency of NBI during the ramp-up, due to reduced plasma electron temperatures. NBI would be capable of driving a large part of the plasma current during this phase, helping in saving the central solenoid flux of DEMO1.

In this paper we discussed DEMO1 NBI system parameters, focusing on injection geometry and energy. The required amount of heating power, crucial to size the system, will be specified in future studies, as a consequence of the ramp-up and ramp-down adopted strategies. Taking into account the recommendations given in this study, an optimized NBI is shown to be an effective heating system for DEMO1 plasma, both for the whole flat-top phase and for a considerable part of the transient phases.

## Acknowledgements

This work has been carried out within the framework of the EUROfusion Consortium and has received funding from the Euratom research and training programme 2014-2018 and 2019-2020 under grant agreement No 633053. This work has been supported also by an EUROfusion Engineering Grant. The views and opinions expressed herein do not necessarily reflect those of the European Commission.

The authors would like to thank the whole Aalto University ASCOT group for the support and guidance received.

## References

[1] G. Federici et al 2019 Nucl. Fusion59 066013
[2] Zohm H. et al., Nucl. Fusion, 57 (2017), 086002
[3] Siccinio M. et al, Fusion Eng. Des. 156 (2020), 111603
[4] R. Wenninger et al., Nucl. Fusion, 57 (2017), p. 016011
[5] P. Vincenzi et al., Fusion Engineering and Design 123 (2017) 473–476
[6] H. Eubank et al., Physical Review Letters 43 (1979) 4

[7] Wagner et al., Physical Review Letters 49 (1982) 1408
[8] Strachan et al. Physical Review Letters 72 (1994) 3526
[9] Keilhacker et al., Nucl. Fusion 39 (1999) 209
[10] V. Antoni et al., Rev. Sci. Instrum. 85 (2014)
[11] T. Franke et al., Ieee Transactions on Plasma Science, vol. 46, no. 5, may 2018
[12] P. Vincenzi et al., "Neutral beam injection for DEMO alternative scenarios", Fusion Engineering and Design accepted (2020)
[13] G. Granucci et al 2017 Nucl. Fusion 57 116009
[14] Dirk Van Eester et al 2019 Nucl. Fusion 59 106051
[15] R. S. Hemsworth, and D. Boilson, AIP Conference Proceedings 1869, 060001 (2017); https://doi.org/10.1063/1.4995788
[16] C. Hopf et al., 2019, Fusion Engineering and Design 146 705–708
[17] A. Komori et al 2010 Fusion Sci. Technol. 58 1–11
[18] D. Bresteau et al., Rev. Sci. Instrum. 88, 113103 (2017)
[19] S.S. Popov et al., 2018 Nucl. Fusion 58 096016
[20] P. Vincenzi et al., 2019, Fusion Engineering and Design 146 1360–1363
[21] E. Surrey and A. Holmes, AIP Conference Proceedings 1515, 532 (2013)
[22] G. Giruzzi et al 2015 Nucl. Fusion55 073002
[23] P. Sonato et al 2017 Nucl. Fusion 57 056026
[24] P. Agostinetti et al., 2020, Fusion Engineering and Design 159 111628
[25] A. Simonin et al, Nucl. Fusion 55 (2015) 123020
[26] K. Watanabe, Fusion Engineering and Design, Volume 49, Issue 6, June 1997, Pages 631-639
[27] A. Kojima, et al., Rev. Sci. Instrum. 81, 02B112 (2010)
[28] J.F. Artaud et al 2018 Nucl. Fusion58 105001
[29] Hirvijoki E. et al. 2014 Computer Physics Communications 185 1310–132
[30] Asunta O. et al 2015 Computer Physics Communications 188 33–46
[31] Varje J. et al., 2019, Fusion Engineering and Design 146 Part B 1615-1619
[32] Kurki-Suonio et al., (2018), Clearing the road for high-fidelity fast ion simulations in full three dimensions. Journal of Plasma Physics, 84(6), 745840603. doi:10.1017/S0022377818000946
[33] Albanese R. et al., 2015 Fusion Engineering and Design, 96-97, pp. 664-667
[34] P. Vincenzi et al., 2017 EPS conference, Belfast P4.146
[35] Wesson John and Campbell David J. Tokamaks. 118. Oxford University Press, 2004
[36] Mitsuru Kikuchi, Karl Lackner, Minh Quang Tran: Fusion Physics. Hrsg.: Internationale Atomenergieagentur, Wien 2012, ISBN 9789201304100
[37] Suzuki S et al 1998 Plasma Phys.Control. Fusion 40 2097
[38] T H Stix. "Heating of toroidal plasmas by neutral injection". In: Plasma Physics 14.4 (1972), p. 367
[39] V. Toigo et al 2019 Nucl. Fusion59 086058
[40] C. D. Challis et al 1989 Nucl. Fusion 29 563
[41] Jenkins I. et al., Fusion Engineering and Design 106 (2016) 9–16
[42] P. Vincenzi et al 2015 Nucl. Fusion55 113028
[43] P. Vincenzi et al, 2019, Nuclear Materials and Energy 18, 188-192
[44] R. Wenninger, et al., Nucl. Fusion 57 (2017) 046002
[45] A.R. Polevoi, et al., Nucl. Fusion 53 (2013) 123026
[46] F. Ryter et al., Nucl. Fusion 54 (2014) 083003
[47] M. Schmidtmayr et al., Nucl. Fusion 58 (2018) 056003
[48] Vincenzi P. et al., 2019 EPS conference, Milano P2.1081
[49] M. Cavedon, "Power losses mechanisms for neutral Beam injected particles in ASDEX Upgrade tokamak under different plasma configurations", 2012, master thesis in Physics, Università degli Studi di Padova